

## Proposal

It is very difficult to utilize the traditional way to drive such a large system. For instance, knee bent walking is a traditional way of bipedal gait; it is 16 times less efficient than humans [1]. In addition, the gravity torque due to the super-size body can easily exceed the physical limits of the actuators. In fact, the larger the knee bent angle, the greater the effective torque acting on the actuators of the lower limbs. These facts induce the importance of human-like motion.

However, most of the technologies utilized in achieving human-like gait are still require a lot of torque compensation at the ankle joint, or some compensatory motions, such as moving waist, swinging arms, etc., which may result in extra energy consumption. Previous research [2] have pointed out that the arm swinging is not an evolutionary relic of quadrupedalism, it is an integral part of the energy economy of human gait. The lack of this swinging motion does not affect the characteristics of normal speed gait. By using the motion of swinging arms to achieve human-like walking may be inconsistent with the facts.

In view of this, a new type mechanism of humanoid robot and relevant process flow of gait were proposed [3] (please see appendix). Unlike the traditional way of changing the center of gravity (CoG) or compensating a torque to move the zero-moment point (ZMP) into the supporting area. The other way is by moving the supporting area to the location of the ZMP to maintain the balance, thus shortening the transverse travel distance of the upper body, decreasing the torque requirement of the actuators of the lower limbs, and reducing redundant work on ZMP compensation. Video [4] shows that even the robot walks in a slow motion, it still can maintain balance and present the characteristics of the human gait.

Nevertheless, the technologies mentioned above are still not enough to let such a huge robot to cope with unexpected ground conditions. Any unexpected ground conditions may make the 18 meters height system fall down. Therefore, not only the mature technology of electronic control must be considered, but also the self-adaptive mechanism should be utilized to deal with the initial position of the foot-ground contact. The technology of the self-adaptive mechanism is being developed (Figure 1). This mechanism now has the ability of automatic processing of the angle variance from the heel-contact to the toe-off. Furthermore, the knowledge of human-like motion [3] has matured. Hope these technologies mentioned above can be adopted by Gundam Global Challenge.

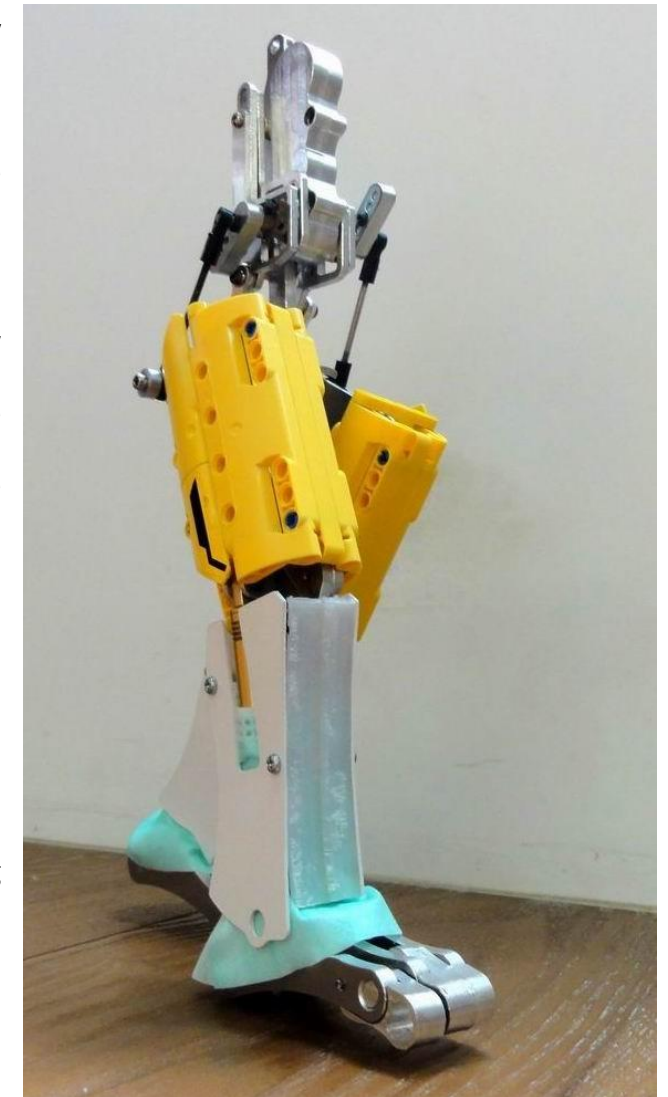


**Figure 1** Prototype of a Robot with the self-adaptive mechanism

## Anthropomorphic Design of the Human-Like Walking Robot

Ming-Hsun Chiang, Fan-Ren Chang

台湾国立大学電子工学学部(台湾、台北) 10617

### Abstract

In this paper, we present a new concept of the mechanical design of a humanoid robot. The goal is to build a humanoid robot utilizing a new structure which is more suitable for human-like walking with the characteristics of the knee stretch, heel-contact, and toe-off. Inspired by human skeleton, we made an anthropomorphic pelvis for the humanoid robot. In comparison with conventional humanoid robots, with such the anthropomorphic pelvis, our robot is capable of adjusting the center of gravity of the upper body by the motion of pelvic tilt, thus reducing the required torque at the ankle joint and the velocity variations in human-like walking. With more precise analysis of the foot mechanism, the fixed-length inverted pendulum can be used to describe the dynamics of biped walking, thus preventing redundant works and power consumption in length variable inverted pendulum system. As the result of the new structure we propose, a humanoid robot is able to walk with human-like gait.

**Keywords:** humanoid robot, anthropomorphic robot, mechanical design, human-like walking, heel-contact motion, toe-off motion

Copyright © 2013, Jilin University. Published by Elsevier Limited and Science Press. All rights reserved.  
doi: 10.1016/S1672-6529(13)60214-0

### 1 Introduction

Many technical articles indicate that because of high homophily with human, humanoid robots are very suitable for practical use in human daily life. Nowadays, many research groups have developed different techniques in creating their own humanoid robots. Among those, HONDA robot ASIMO<sup>[1]</sup> is the best-known, and the techniques it utilizes is widely referenced by researchers. With the floor reaction control, the target Zero Moment Point (ZMP)<sup>[2]</sup> control, and the foot planting location control, ASIMO can achieve stable walking, running, and stairs-climbing, *etc.* However, the innate structure of the ASIMO, particularly without a pelvis, leads to difficulties in achieving human-like walking. During long stride or faster walking, the overall height of ASIMO is greatly reduced with much larger walking spans than ones capable of knee-stretch walking. The reduced height is not as suitable for interaction with human, as it was originally proposed. This highlights the importance of stretched knees in achieving human-like walking in a humanoid robot. In developing humanoid robots with stretched knees walking, both WABIAN-2R<sup>[3]</sup> of Waseda University and HRP-4C<sup>[4]</sup> of Advanced In-

dustrial Science and Technology (AIST) show very impressive results. They both prove that a humanoid robot must have a two Degree-of-Freedom (DOF) waist compensatory motion to maintain balance during human-like walking. However, performing such a walk with stretched knees requires a high torque at the ankle joint<sup>[5]</sup> and rapid changes in velocity in order to maintain balance, which may mean more power consumption.

In order to reduce rapid changes in velocity, the burden at the joint, we utilize the anthropomorphic pelvis to do the motion of pelvic tilt, which has been regarded useless in walking by the research group of Wabian-2R of Waseda University<sup>[6]</sup>. According to motion analysis, we understand that pelvic tilt motion can help human or humanoid robot by adjusting the Center Of Gravity (COG) of the upper body as it needs, so that the ZMP will stay in the supporting area more easily, thus reducing the dependence on the ZMP control which consumes more power by generating acceleration. Fewer changes in velocity mean less power consumption.

Most of the conventional bipedal robots are modeled as a 3D inverted pendulum, the length of which is variable and controllable to ensure the height of the robot's COG is a constant. However, the human bipedal

**Corresponding author:** looka330@gmail.com  
**E-mail:** Ming-Hsun Chiang

walk is a series of falls and recoveries. The difference is that the latter has very little length variation of the supporting leg, which means less energy consumption. By imitating human walking, we utilize fixed-length inverted pendulum instead of length variable inverted pendulum to describe the dynamics of bipedal walking. Through creating a miniature humanoid robot, this paper serves to proof the ideas mentioned above.

### 2 Design concept

Although some humanoid robots can achieve human-like walking with knee stretch, heel-contact, and toe-off motion in present days, they still require a lot of torque compensation at the ankle joint, or some compensatory motions, such as moving waist, waving arms, *etc.*, to achieve such walking gaits. The methods mentioned above compensate the ZMP mostly by creating rapid changes of velocity<sup>[5]</sup>. We hope to build a humanoid robot inspired by understanding the structure of human skeleton. The goal is to create robots that will achieve human-like walking and reduce their dependency on the torque compensation, or compensatory motion while they walk.

#### 2.1 Overview of mechanical design

Fig. 1 shows the robot we developed in this study. For the material lightweight and stiffness, we use aluminum alloy as the base material of the exoskeleton of the robot. Table 1 shows the main specifications of the robot. Fig. 2 shows the DOF configuration of the robot. The inertial coordinate system fixed on the ground with rotational directions indicates the movement of each joint. As shown in Fig. 2 and Table 2, this robot has a 3-DOF waist in the pelvis, a 3-DOF trunk, and a pair of 3-DOF hips, 5-DOF legs, and of 5-DOF arms. The 3-DOF waist joint in the back of pelvis is composed of roll axis, yaw axis, and pitch axis. These three axes should be perpendicular to each other, with intersection of lying in the median sagittal plane, and higher than the hip joints. In other words, the frontal plane of the lower-body is in front of the one of the upper-body. This characteristic results in the reduction for the need for compensation along the track direction when the robot walks. In addition, the distance between two knees should be smaller than the distance between two hip joints while the robot stands straight. This characteristic will reduce the need of compensation in frontal plane

when the robot walks. Unlike the large hip extension Range of Motion (ROM) of the current robots, the hip extension ROM of human is just about 15°<sup>[7]</sup>. The robot in this paper was designed to follow this finding.

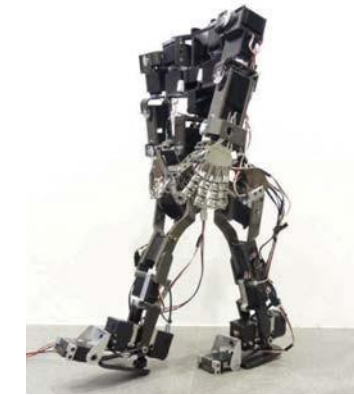


**Fig. 1** Photograph of the robot with anthropomorphic pelvis.

**Table 1** Principal specifications of the robot in this paper

Weight and measurements	Value
Weight	3.5 (kg)
Height	531 (mm)
Width	288 (mm)
Depth	169 (mm)

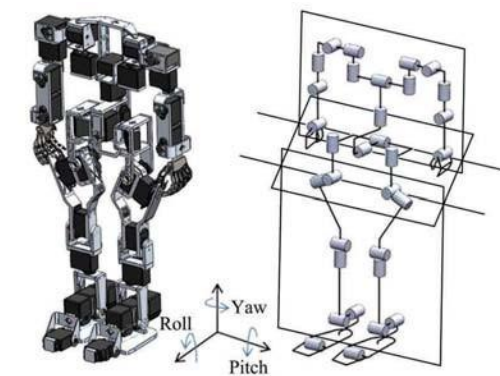


**Fig. 2** The DOF configuration.

**Table 2** The DOF assignment

Position	Total 32 DOF
Arm	2 Arms × 4 = 8 DOF
Hand	2 Hands × 1 = 2 DOF
Torso	1 Torso × 3 = 3 DOF
Waist	1 Waist × 3 = 3 DOF
Hip	2 Hips × 3 = 6 DOF
Leg	2 Legs × 5 = 10 DOF

#### 2.2 Close-up of the pelvis

Fig. 3 shows the superior view and frontal view of human's pelvis. As shown in the figure, the acetabulum

has a concave surface at the lower front part of both sides of the pelvis. The femur head fits into the pelvis at the acetabulum, forming the hip joint. The sacroiliac joint connects the ilium and sacrum at the upper rear part of the pelvis. The motions of the sacroiliac joint include the anterior pelvic tilt and the posterior pelvic tilt. If the motions of spine are taken into account, human can move the pelvis in 3 directions: yaw, roll, and pitch. According to the relative position of these joints on pelvis, a cross-sectional view of the anthropomorphic pelvis was designed as shown in Fig. 4. To simplify the design, we combined the functions of the spine and the sacroiliac

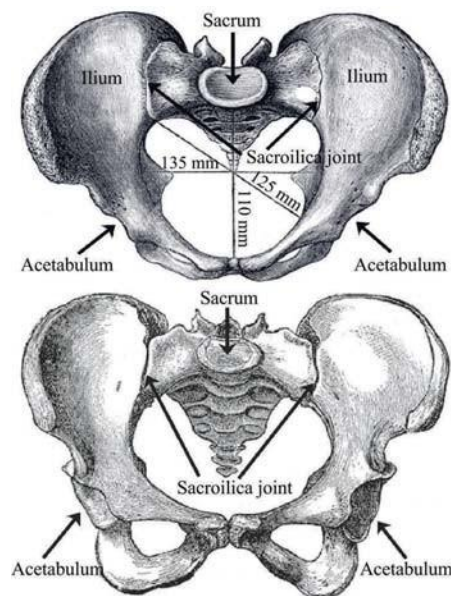


Fig. 3 Superior view and frontal view of the human pelvis (Drawings are cited from Ref. [9]).

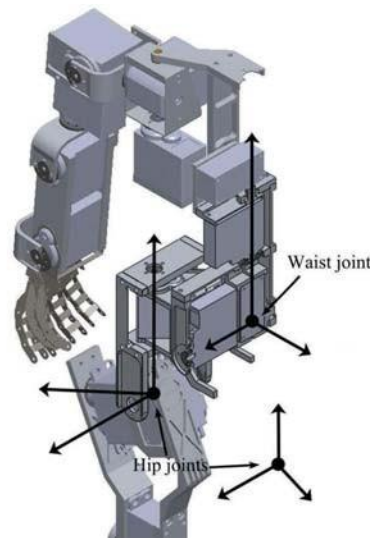


Fig. 4 Cross-section view of the anthropomorphic pelvis.

joint to a 3-DOF waist joint. The waist joint is located at the upper rear side of the middle point between the two hip joints. The advantage of a robot with such an anthropomorphic pelvis is that the ZMP can stay in the range of supporting foot more easily while walking, therefore reduce its reliance on the torque compensation.

### 3. Functionality of the pelvis in human-like walking

The functionalities of the pelvis in human-like walking are discussed as follows.

(1) Forming a lever arm: Fig. 5a shows that if a conventional robot performs the single hip flexion, gravity force on its raising leg will provide a falling torque. Fig. 5b shows that a robot with the anthropomorphic pelvis can be viewed as a lever system instead, where the hip joint of the supporting leg is the fulcrum; the upper body provides an anti-torque mechanism for the raising leg. This design provides a better balance than the design used in conventional robot in single-leg supporting phase.

(2) Providing extra DOFs to change the position of upper-body's COG: When a walking robot is in the state of zero acceleration with two-leg supports, its ZMP is within the supporting polygon area, but shifts out of the range of the feet. A situation like this is one of the main technical issues in human-like walking to compensate the ZMP into the front foot before the robot transits to a single-leg supporting state. In comparison with the conventional robot (Fig. 6a), a robot with anthropomorphic pelvis has extra DOFs to change the position of upper-body's COG by creating the pelvic tilt and keeping the upper-body upright simultaneously (Fig. 6b). We know that the location of the ZMP will also change accordingly.

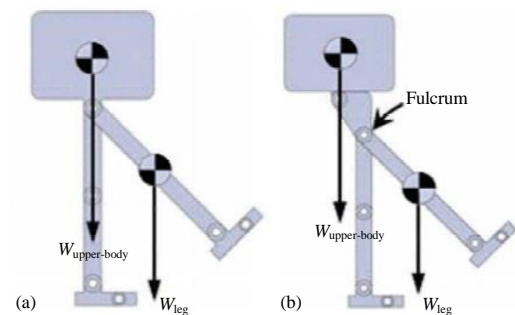


Fig. 5 Single hip flexion. (a) Gravity force on conventional robot's raising leg provides a falling torque; (b) because of the anthropomorphic pelvis, the weight of the upper body becomes a counterweight to the raising leg.

While a walking robot is under the two-leg supporting state, a conventional one walks with one hip flexed, and another hip extended. Our robot walks with both hips flexed, and anterior pelvic tilted. In the past, researchers pointed out the relationship between the motion of anterior pelvic tilt and running<sup>[9]</sup>. They further found that, even when human being performs running, the average hip extension flexibility value is just about 17.4°. However, the range of motion of hip extension designed for conventional robots is much larger than that of human beings. Obviously, the way conventional robots built for walking is very different from that of human beings. Humans and robots with anthropomorphic pelvis can utilize the motions of anterior pelvic tilt and toe-off correctly, thus bringing the ZMP into the front foot easily. It is very difficult for conventional robots to do the same thing, unless they utilize the method of torque compensation. The more torque compensation a robot needs in walking means the more power consumption.

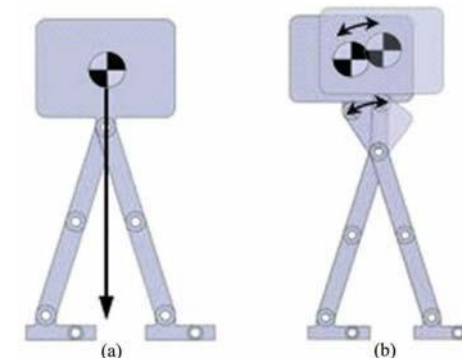


Fig. 6 Two-leg supporting state. (a) The position of conventional robot's upper body is hard to change; (b) a robot with anthropomorphic pelvis has extra DOFs to change the upper body position.

### 2.4 Standing pelvic tilt

The COG of a human is slightly below the belly button<sup>[10]</sup>, in front of the sacrum, and at about the second sacral level. Following this fact, the COG of the robot is designed in the front of and at the same height as the waist joint when standing up. The disadvantage of a robot with the anthropomorphic pelvis is that it is more prone to fall backwards than the conventional robot while standing straight (Fig. 7a). However, this problem can be easily resolved with the motion of anterior pelvic tilt, as shown in Fig. 7b. The position in Fig. 7b is called as Standing Pelvic Tilt (SPT). It is the same as that of human beings<sup>[11]</sup>.

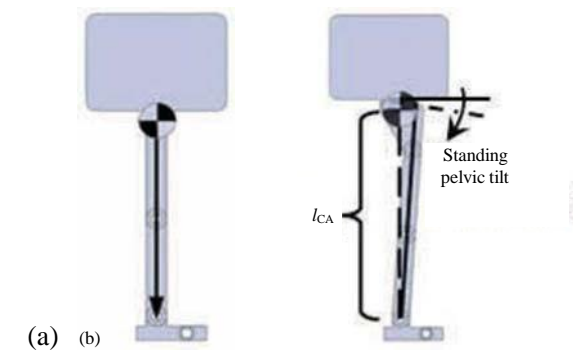


Fig. 7 Standing position. (a) Projection of the COG of the conventional robot is in the range of the feet while standing straight; (b) projection of the COG of the robot with anthropomorphic pelvis keeps within the feet through the motion of pelvic tilt.

### 3 Robot walking

The length variable dynamics used in describing the bipedal walking can be written as

$$\begin{cases} ml^2\ddot{\theta} - mgl \sin\theta + 2ml\dot{\theta} = \tau \\ m\ddot{l} + mg \cos\theta - ml\dot{\theta}^2 = f \end{cases}, \quad (1)$$

where  $m$  is the mass of the robot,  $l$  is the length from the COG to the Center Of Pressure (COP),  $g$  is the acceleration due to gravity,  $f$  is the ground reaction force,  $\theta$  is the angle between the equilibrium position and the pendulum, and  $\tau$  is the torque exerted on the pivot. Furthermore, with more precise analysis of the vertical distance between the ankle joint and the toe joint, the variable-length inverted pendulum problem will then become a fixed-length inverted pendulum problem instead. The walking pattern is based on COP switched<sup>[12]</sup>. To accomplish one step period, a robot will go through four stages. The beginning position of the COG in every stage is a relatively high position except the recovery stage. The detail is mentioned below. For simplification, the conditions mentioned below are under zero acceleration.

The first stage is the lifting of the swing leg, as shown in Fig. 8a. The weight of the swing leg provides a torque that makes the robot lean forward until the COG crosses above the pitch axle of the toe joint. The pitch-direction ankle joint is the pivot, and  $l_{CA}$  (from the COG to ankle joint) is the length of the pendulum. The height reduction of the COG in this stage is

$$l_{CC} = l_{CA}(1 - \cos\theta_1). \quad (2)$$

The angle swing in this stage is

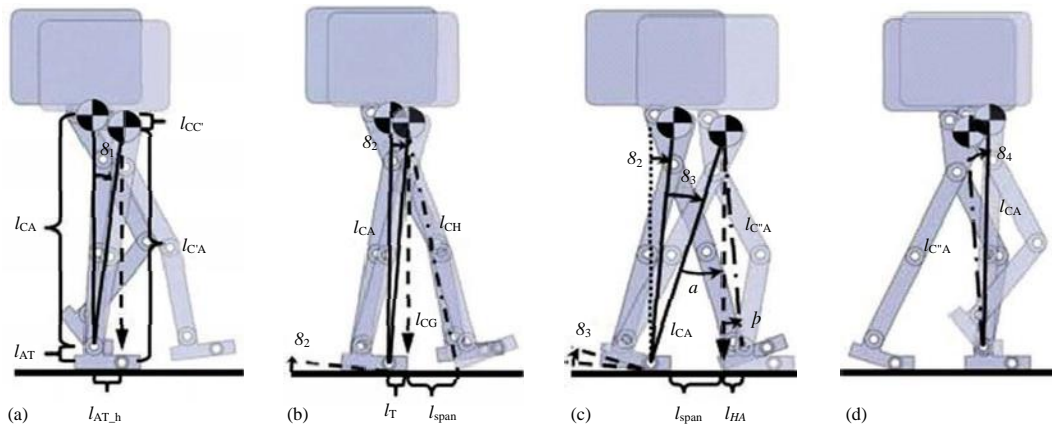


**Fig. 8** (a) The lifting of the swing leg stage; (b) the toe-off and heel-contact stage; (c) the toe-off and entire foot landing stage; (d) the recovery stage (The light colored part denotes the end of the stage and the beginning of the next stage).

$$\theta_1 = \sin^{-1} \left\{ \frac{l_{AT\_h}}{l_{CA}} \right\}, \quad (3)$$

where  $l_{AT\_h}$  is the horizontal distance between the ankle joint and the toe joint.

The second stage is the toe-off and heel-contact, as shown in Fig. 8b. The pivot in this stage is switched to the toe joint. If the vertical distance between the ankle joint and the toe joint  $l_{AT}$  is designed to equal  $l_{CC}$ , then the length of the pendulum in this stage is also equal to  $l_{CA}$ . The pitch angle of the supporting ankle joint is fixed at  $\delta_1$ . The robot rotates the pitch axle of the supporting toe joint which will lead the COG to fall downwards continuously. This motion remains until the COG crosses above the tiptoe of the supporting leg, and the heel contact event must occur on the swing leg at the same moment. The angle of inverted pendulum swing in this stage is equal to the angle of supporting toe joint rotation, it can be calculated as

$$\theta_2 = \sin^{-1} \left\{ \frac{l_T}{l_{CA}} \right\}, \quad (4)$$

where  $l_T$  is the length of the toe. The length from the contact point to the COG is equal to

$$l_{CH} = \sqrt{l_{span}^2 + l_{CG}^2}, \quad (5)$$

where  $l_{span}$  is the distance of span,  $l_{CG}$  is the vertical distance from the COG to the ground.

The third stage is the changing of the supporting leg, as shown in Fig. 8c. The pivot in this stage is the toe joint of the trailing leg, and the point of the leading heel contacts with the ground is the other. The toe-off motion

continues until the leading foot touches the ground entirely.  $\delta_3$ , the angle of inverted pendulum swings in this stage, which is equal to the angle of supporting toe joint rotation. At this moment, the projection of COG on the ground must in the range of the leading foot, that is

$$l_{CA} \sin(\theta_2 + \theta_3) > l_T + l_{span}. \quad (6)$$

Hence

$$\theta_3 > \sin^{-1} \left\{ \frac{l_T + l_{span}}{l_{CA}} \right\} - \theta_2, \quad (7)$$

in which,  $a$  is equal to  $\delta_2 + \delta_3$ , and  $b$  is

$$J < \tan^{-1} \left\{ \frac{l_{HA}}{l_{CA} \cos(\theta_2 + \theta_3) - l_{AT}} \right\}, \quad (8)$$

in which,  $l_{HA}$  is the horizontal distance between the heel and the ankle joint. The length from the ankle joint of the leading leg to the COG is

$$l_{CA'} = [l_{CA} \cos(\theta_2 + \theta_3) - l_{AT}] \sec(J). \quad (9)$$

The fourth stage is the recovery, as shown in Fig. 8d. The trailing leg raises and starts to swing. The length of the leading leg  $l_{CA'}$  is stretch to  $l_{CA}$ . The rotation angle  $\delta_4$  is

$$\theta_4 = \sin^{-1} \left\{ \frac{l_{HA}}{l_{CA'}} \right\}. \quad (10)$$

The COG is pushed to the high point by the supporting leg.

These four stages constitute one step. By repeating stage 1, 2, 3, 4 with another leg as stage 5, 6, 7, 8, it forms a complete walk cycle.

#### 4 Discussion

By fixing the length of the inverted pendulum, the derivative term of  $l$  in dynamic equation will be vanished. Eq. (1) will be reduced to

$$\begin{cases} ml^2 \ddot{\theta} - mgl \sin \theta = \tau \\ mg \cos \theta - ml \dot{\theta}^2 = f \end{cases} \quad (11)$$

In comparison with Eq. (1), Eq. (11) shows that less torque is needed on fixed-length inverted pendulum system. From the point of constant compensating energy control<sup>[13]</sup>, the energy input in every walk cycle is

$$E_{in} = \int f l_{span} d\theta_4, \quad (12)$$

where  $f$  denotes the ground-pushing force along the inverted pendulum axis of the trailing leg. Eq. (11) and Eq. (12) show that less energy is needed in the fixed-length inverted pendulum system. Besides, the fixed-length inverted pendulum also prevents the extra power consumption from the length variation during the first stage to the third stage, which was known as

$$\int f l dt, \quad (13)$$

where  $F$  denotes the force along the axis of the inverted pendulum,  $l$  is the effective length of the supporting leg.

According to the principle in section 3, each joint angle in a walk cycle can be positively given. In this paper, the time of every stage is set to be one second. The information of every joint angle is fed per second. The function spline in MATLAB is used to approximate the data set. The angle variation of the pelvis and the hip are shown in Fig. 9 and Fig. 10, respectively.

For the conventional robot, the hip flexion-extension angle has usually been treated as the leg swing angle, but the pelvic tilt does affect the leg swing angle. The real leg swing angle is subtracting the pelvic tilt angle (Fig. 9) from the hip flexion angle (Fig. 10), the result is shown in Fig. 11. Similar curve like that in

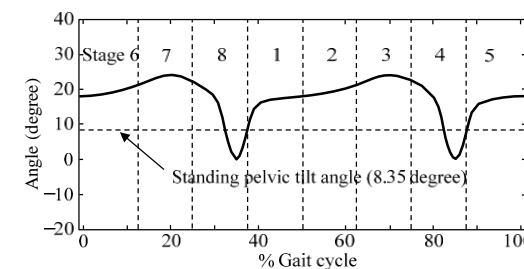


**Fig. 9** Pelvic tilt in sagittal plane of the robot in a gait cycle.

Fig. 11 can be easily found in most of the technical issues in the field of the gait research<sup>[14-17]</sup>. Fig. 12 shows the joint angle of the human hip in a gait cycle<sup>[17]</sup>.

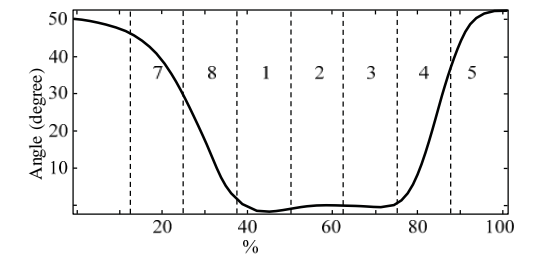


**Fig. 10** Hip flexion of the robot in a gait cycle.

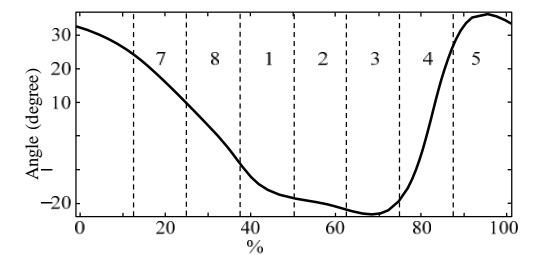


**Fig. 11** Leg motion in sagittal plane of the robot in a gait cycle.

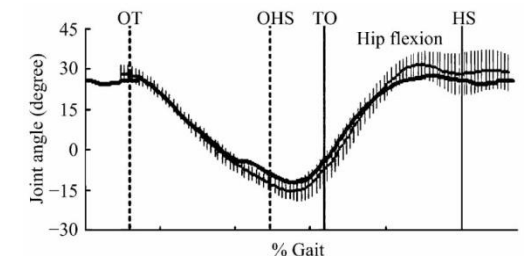


**Fig. 12** Joint angle of the human hip in a gait cycle<sup>[17]</sup>.

#### 5 Motion gallery

Fig. 13 shows that our robot performs a simple dance to demonstrate some pelvic motions, including pitch (pelvic tilt), roll (pelvic obliquity), and yaw (pelvic rotation).

Fig. 14 shows how our robot completes a walk cycle. In this walk scenario, the projection of COG on the ground is considered as the ZMP; in other words, the robot goes through the stages mentioned above with zero torque compensation and still keeps a walk span. From this figure, we can see that the robot could achieve human-like motions of knee stretched, toe-off, and heel contact.

Fig. 15 shows the robot is operated near the maximum angle of heel-contact and toe-off. From Fig. 14 and Fig. 15, we can see that the toe-off event and the heel-contact event have an overlapping time period.

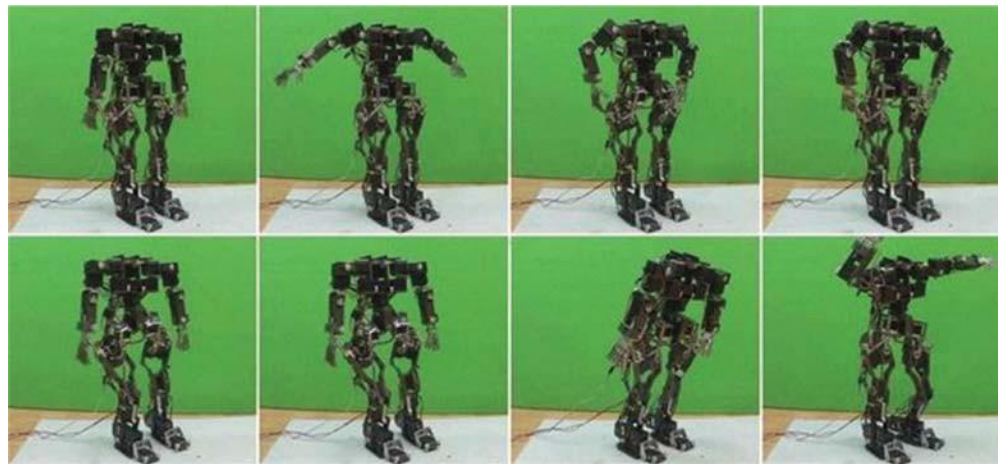


Fig. 13 A simple dance motion.

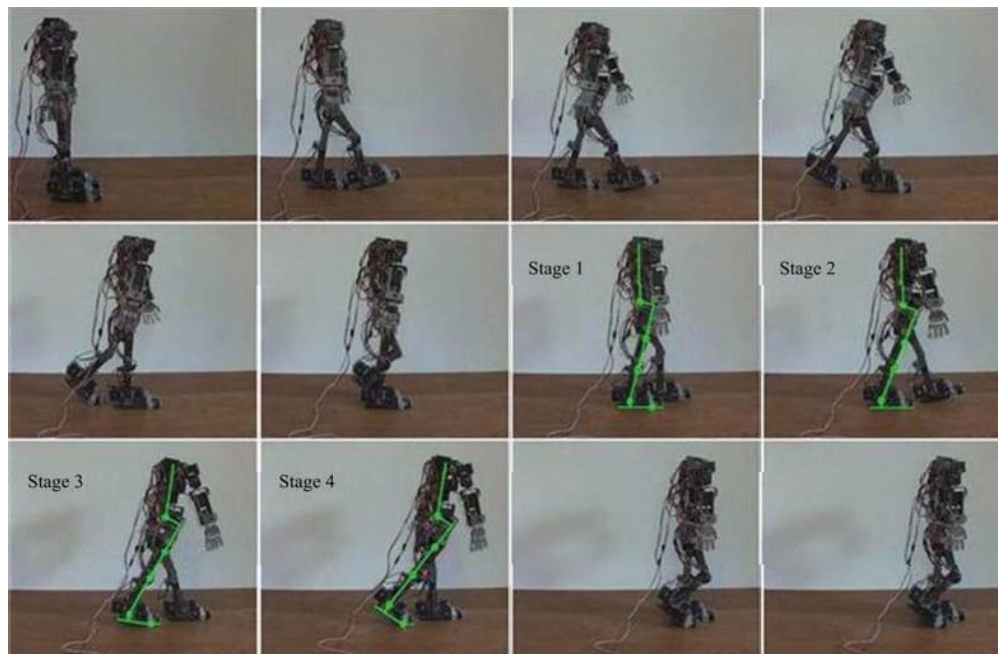


Fig. 14 A normal walking motion.



Fig. 15 A walk motion near the limit angle of heel-contact and toe-off.

## 6 Conclusion

For conventional robot, because of the violent change of the supporting area between two-leg and single-leg supporting, one of the main technical issues in human-like walking is to enable the ZMP of the robot to be compensated into the front foot prior to raising its rear leg during a walk cycle. Inspired by human skeleton structure, we claimed that the anthropomorphic pelvis and pelvic tilt motion in sagittal plane must be considered in humanoid robot design and walk. Because of the innate structure of the anthropomorphic pelvis, the ZMP could be kept in the supporting area easily while single-leg lifting. In addition, the anthropomorphic pelvis provides the tilt DOF to change the location of the ZMP along the track direction. Hence the ZMP is able to stay in the range of the supporting foot easily, thus reducing redundant work on ZMP compensation. Integrate the concepts mentioned above, the robot present in this paper could achieve the human-like gait with the characteristics of knee-stretch, toe-off, and heel-contacts, and an additional advantage is that it consumes less energy. Furthermore, the ZMP of the robot is easier to control than the conventional robot. Now that the technologies in developing ZMP compensation have matured, we believe that the concepts we proposed will help bringing the human-like walking of the robots into a new phase.

## References

- [1] Hirai K, Hirose M, Haikawa Y, Takenaka T. The development of Honda humanoid robot. *Proceeding of the IEEE International Conference on Robotics and Automation (ICRA)*, Leuven, Belgium, 1998, 1321–1326.
- [2] Vukobratovic M, Brovac B, Surla D, Stokic D. *Biped Locomotion: Dynamics, Stability, Control and Application*, Springer-Verlag, New York, USA, 1990.
- [3] Ogura Y, Shimomura K, Kondo H, Morishima A, Okudo T, Momoki S, Lim H, Takanishi A. Human-like walking with knee stretched, heel-contact and toe-off motion by a humanoid robot. *Proceeding of the 2006 IEEE/RSJ International Conference on Intelligent Robot and Systems (IROS)*, Beijing, China, 2006, 3976–3981.
- [4] Kaneko K, Kanehiro F, Morisawa M, Miura K, Nakaoka S, Kajita S. Cybernetic Human HRP-4C. *Proceeding of the 2009 IEEE-RAS International Conference on Humanoid Robots*, Paris, France, 2009, 7–14.
- [5] Omer A, Ghorbani R, Lim H, Takanishi A. Semi-passive dynamic walking for humanoid robot using controllable spring stiffness on the ankle joint. *Proceedings of the 2009 4th International Conference on Autonomous Robots and Agents*, Wellington, New Zealand, 2009, 681–685.
- [6] Kondo H, Ogura Y, Shimomura K, Momoki S, Okubo T, Lim H, Takanishi A. Emulation of human walking by biped humanoid robot with heel-contact and toe-off motion. *Journal of Robotics and Mechatronics*, 2008, **20**, 739–749.
- [7] Lee H M, Moroz A. Physical Therapy. [2013-03], [http://www.merckmanuals.com/professional/special\\_subjects/rehabilitation/physical\\_therapy\\_pt.html](http://www.merckmanuals.com/professional/special_subjects/rehabilitation/physical_therapy_pt.html)
- [8] Gray H. The Pelvis. [2013-03], <http://www.bartleby.com/107/58.html>
- [9] Schache A G, Blanch P D, Murphy A T. Relation of anterior pelvic tilt during running to clinical and kinematic measures of hip extension. *British Journal of Sports Medicine*, 2000, **34**, 279–283.
- [10] Elert G. Center of Mass of a Human. [2013-03], <http://hypertextbook.com/facts/2006/centerofmass.shtml>
- [11] Gajdosik R, Simpson R, Smith R, DonTigny R L. Pelvic tilt. Intratester reliability of measuring the standing position and range of motion. *Journal of the American Physical Therapy Association*, 1985, **65**, 169–174.
- [12] Lou X, Li W, Zhu C. Planning and control of COP-switch-based planar biped walking. *Journal of Bionic Engineering*, 2011, **8**, 33–48.
- [13] Lou X, Guo R, Zhu C. An orbit based control for biomimetic biped walking. *Proceeding of IEEE International Conference on Robotics and Biomimetics*, Guilin, China, 2009, 19–23.
- [14] Lou X, Xu W. Planning and control for passive dynamics based walking of 3D biped robots. *Journal of Bionic Engineering*, 2012, **9**, 143–155.
- [15] Xiang Y, Arora J S, Abdel-Malek K. Optimization-based prediction of asymmetric human gait. *Journal of Biomechanics*, 2011, **44**, 683–693.
- [16] Lister S J, Jones N B, Spurgeon S K, Scott J J A. Simulation of human gait and associated muscle activation strategies using sliding-mode control techniques. *Journal of Simulation Modeling Practice and Theory*, 2006, **14**, 586–596.
- [17] Fernandez J W, Pandy M G. Integrating modeling and experiments to assess dynamic musculoskeletal function in humans. *Experimental Physiology*, 2006, **91**, 371–382.